Photo-Auger-ionization and charge-state distribution

Gaber Omar
Department of Physics, Ain Shams University, Abbassia, Cairo, Egypt

Yukap Hahn
Department of Physics, University of Connecticut, Storrs, Connecticut 06269
(Received 4 September 1990)

The radiative and Auger emissions in cascade (RAC) model constructed earlier [G. Omar and Y. Hahn, Phys. Rev. A (to be published)] is applied to the calculation of the final-charge-state distribution in the decay of $Ar^+(\overline{1s})$ with an initial $1s$ hole created by synchrotron irradiation. Experimental data of Church *et al.* [Phys. Rev. A **36**, 2487 (1987)] are reasonably well reproduced, including the observed asymmetry in the final-state charge distribution. In addition to $Ar^+(\overline{1s})$, we have also considered the decay of the initial states $Ar^+(\overline{2s})$, $Ar^+(\overline{2p})$, and $Ar(\overline{1s},4p)$. The higher charge states are underestimated by the RAC model, presumably due to the neglect of correlated multielectron processes in the present calculation.

I. INTRODUCTION

Much useful information on exotic ions can be obtained by observing the decay of hollow ions with one or more inner-shell holes in the initial state. Such ions may be created by synchrotron irradiation [1–5] of a target ion, or by electron and ion impact on target gases. In addition, an ion-surface interaction [6] may also produce hollow ions with many inner-shell vacancies.

When these ions decay by emitting photons and/or Auger electrons sequentially in a cascade, many new intermediate states of ions are produced. At each stage of the decay process, there are many decay channels available for these intermediate states to follow, until stable final states are reached, with the final-state charge Z_f. Obviously, the probability $P(Z_f,Z_i)$ for the final charge state with Z_f depends [7,8] on the branching ratios (fluorescence yield ω, and Auger yield ξ) for each intermediate state an ion passes through. The radiative and Auger emissions in cascade (RAC) model proposed recently [9] assumes that the distribution P depends only on the relevant ω and ξ. Thus, the effects of collective shake-off, correlated two-electron transitions, post-collision interactions among the slow-fast Auger electrons, etc., are neglected in this model, although such processes, which are present for ions with many electrons in the outer shells, can provide higher charge states than that predicted by the RAC. In fact, the present work should shed light on the role of these alternate modes.

A consistent theoretical treatment of correlated multielectron (CME) processes is difficult, and no reliable procedure is currently available to incorporate the CME effect in the RAC formalism. The usual procedure of estimating the shake-off contribution by taking the overlap of the wave functions before and after the inner-shell transition in a sudden approximation is inadequate here, mainly because of the serious double-counting problem. Attempts have been made in the past to derive reliable three-electron vertices, with little success. This problem is a difficult one and a subject of much current activity.

In this paper, we apply the RAC model to $Ar^+(\overline{n_i l_i})$ and examine its validity by comparing the prediction with experimental data of Church *et al.* [3]. The calculation is very lengthy and tedious, but rather straightforward; for example, there are many intermediate states involved in the decay of the $1s$ hole. It is possible that the initial holes created may involve excitations of different electron orbitals, as is often the case in electron-ion and ion-atom collisions. In such cases, the final-charge-state distribution may be given by a superposition of the states $\overline{1s},\overline{2s},\overline{2p},\ldots$. On the other hand, when two or more holes are created simultaneously, the superposition scheme is no longer valid.

Unique to the photon-target collision processes, as contrasted to the ion-target collision for example, is the fact that the photon-electron coupling is mainly a one-electron operator. Therefore, under the single-collision condition, the photon will be absorbed by one of the electrons, moving to an excited or to a continuum state. Transitions in which two or more orbitals are changed require strong configuration mixing. In the case of high-energy ion-target collisions, however, the condition for single-electron transitions is more difficult to realize in practice, especially when deep inner-shell vacancies are to be created with large energy deposition. Hence, more selective excitations of the inner-shell electrons may be possible with a well-collimated photon beam. Specifically, with synchrotron irradiation, the hole creation is somewhat more precise in the sense that one electron is excited at a time.

As noted previously, the present calculation not only provides a check on the validity of the RAC, but also isolates the effect of the CME processes, which are neglected in this calculation. Furthermore, based on this study, a simpler approach may be developed to treat more complex ions [4], such as Kr and Xe.

II. THE RAC MODEL

The complex decay routes of ions with specified initial holes are described in the simple radiative and Auger emissions in cascade (RAC) model. The decay process to be examined is given schematically,

$$
\begin{array}{ccccccc}
\mathrm{Ar}^{+}(\mathrm{d}) & \rightarrow & \mathrm{Ar}^{2+}(\mathrm{d}_{11})+e_1 & \rightarrow & \mathrm{Ar}^{3+}(\mathrm{d}_{21})+e_2 & \rightarrow \cdots \\
\downarrow & & & & \downarrow & \\
\mathrm{Ar}^{+}(\mathrm{d}_{12})+\gamma & \rightarrow & \mathrm{Ar}^{2+}(\mathrm{d}_{22})+e_3 & \rightarrow \cdots & \mathrm{Ar}^{3+}(\mathrm{d}_{31})+\gamma & \rightarrow \cdots \\
\downarrow & & \downarrow & & \downarrow & \\
\mathrm{Ar}^{+}(\mathrm{d}_{23})+\gamma & \rightarrow \cdots & \mathrm{Ar}^{2+}(\mathrm{d}_{33})+\gamma & \rightarrow \cdots & \mathrm{Ar}^{3+}(\mathrm{d}_{41})+\gamma & \rightarrow \cdots \\
 & & \downarrow & & & \\
 & & \mathrm{Ar}^{2+}(\mathrm{d}_{42})+\gamma & \rightarrow & \mathrm{Ar}^{3+}(\mathrm{d}_{51})+e_4 & \rightarrow \cdots \\
 & & & & \downarrow & \\
 & & & & \mathrm{Ar}^{3+}(\mathrm{d}_{61})+\gamma &
\end{array}
$$

where $\overline{n_k l_k}$ implies the kth hole in the $n_k l_k$ orbital, and d_{ij} denotes the channel j in the ith stage of the cascade chain. States d_{11} and d_{12} of the first generation ($i=1$) are unstable and will further decay through Auger emission, producing Ar^{3+}, and so on. The probabilities of reaching d_{ij} from d are given in terms of the Auger and radiative decay probabilities A_a and A_r, respectively, as the respective partial branching ratios

$$\omega(\mathrm{d}\rightarrow \mathrm{d}_{1j})=\frac{A_r(\mathrm{d}\rightarrow d_{1j})}{\Gamma(\mathrm{d})} \tag{1}$$

and

$$\xi(\mathrm{d}\rightarrow \mathrm{d}_{1j})=\frac{A_a(\mathrm{d}\rightarrow \mathrm{d}_{1j})}{\Gamma(\mathrm{d})} , \tag{2}$$

where $\Gamma(\mathrm{d})$ is the total width of state (d) and given in terms of the Auger and radiative decay probabilities A_a and A_r, respectively, as

$$\Gamma(\mathrm{d}_{ij})=\sum_l A_a(\mathrm{d}_{ij}\rightarrow d_{i+1\,l})+\sum_k A_r(\mathrm{d}_{ij}\rightarrow \mathrm{d}_{i+1\,k}) . \tag{3}$$

The final-charge-state probability $P(Z_f,Z_i)$, with the final charge Z_f and the initial state Z_i, is given by

$$\begin{aligned} P(Z_f,Z_i)&\equiv f(Z_f) \\ &=\sum_\alpha F_\alpha(Z_f;\alpha=p_i,q_i) , \end{aligned} \tag{4}$$

where label α denotes the particular cascade path followed in reaching the final charge states Z_f; in general there is more than one path leading to Z_f, hence

$$F_\alpha=\prod_{i=1}^{Z_f-Z_i}(\omega^{p_i}\xi^{q_i}) , \tag{5}$$

where ω and ξ as well as p_i and q_i are explicitly dependent on α, and assume integer values

$$p_i=0,1,2,\ldots , \tag{6}$$

$$q_i=1,2,3,\ldots , \tag{7}$$

with the following constraints:

$$\sum_k q_k=Z_f-Z_i . \tag{8}$$

For example, p_k implies successive p_k Auger decays without radiation in the α chain. The compact notation used for the radiative and Auger cascade branching ratios implies more explicitly

$$\omega^{p_i}\equiv\omega(S_{p_i}\rightarrow S_{p_i-1})\omega(S_{p_i-1}\rightarrow S_{p_i-2})\cdots\omega(S_1\rightarrow f) , \tag{9}$$

$$\xi^{q_i}\equiv\xi(S_{q_i}\rightarrow S_{q_i-1})\xi(S_{q_i-1}\rightarrow S_{q_i-2})\cdots\xi(S_1\rightarrow g) . \tag{10}$$

The number of terms in these branching ratios [Eqs. (9) and (10)] depends also on the available electrons which lie above the holes contained in state s.

In the following, the charge probability P is evaluated in the angular-momentum-average (AMA) scheme described previously [10,11]. In view of the extreme complexity of the calculation involved, the AMA is a reasonable first step. Nevertheless, we expect the final P to be rather insensitive to the coupling scheme, since P is obtained from [12] ω and ξ, which, are constructed as ratios of A_a and A_r, and not from A_a and A_r individually.

III. RESULTS

A. $Ar^{+}(\overline{1s})$

This is the most complex case involving Ar^{+}, with one inner-shell hole. (A somewhat more involved case of $Ar^{0+}(\overline{1s},4p)$ will be treated in the next section). For the initial configuration

$$(\mathrm{d})\equiv 1s2s^2 2p^6 3s^2 3p^6 ,$$

we consider the following Auger and radiative channels leading to the first generation of decay products. The branching ratios for this generation from the initial parent state (d) are given below:

Auger channel	Branching ratio	
$1s^2 2p^6 3s^2 3p^6 + k(l_c=0)$,	$\xi(\mathrm{d}\rightarrow\mathrm{d1})=0.0691$	(d1)
$1s^2 2s 2p^5 3s^2 3p^6 + k(l_c=1)$	$\xi(\mathrm{d}\rightarrow\mathrm{d2})=0.201$	(d2)
$1s^2 2s 2p^6 3s 3p^6 + k(l_c=0)$	$\xi(\mathrm{d}\rightarrow\mathrm{d3})=0.0134$	(d3)
$1s^2 2s 2p^6 3s^2 3p^5 + k(l_c=1)$	$\xi(\mathrm{d}\rightarrow\mathrm{d4})=0.0167$	(d4)
$1s^2 2s^2 2p^4 3s^2 3p^6 + k(l_c=0,2)$	$\xi(\mathrm{d}\rightarrow\mathrm{d5})=0.482$	(d5)
$1s^2 2s^2 2p^5 3s 3p^6 + k(l_c=1)$	$\xi(\mathrm{d}\rightarrow\mathrm{d6})=0.0175$	(d6)
$1s^2 2s^2 2p^5 3s^2 3p^5 + k(l_c=0,2)$	$\xi(\mathrm{d}\rightarrow\mathrm{d7})=0.0719$	(d7)
$1s^2 2s^2 2p^6 3p^6 + k(l_c=0)$	$\xi(\mathrm{d}\rightarrow\mathrm{d8})=0.0007$	(d8)
$1s^2 2s^2 2p^6 3s 3p^5 + k(l_c=1)$	$\xi(\mathrm{d}\rightarrow\mathrm{d9})=0.0015$	(d9)
$1s^2 2s^2 2p^6 3s^2 3p^4 + k(l_c=0,2)$	$\xi(\mathrm{d}\rightarrow\mathrm{d10})=0.0029$	(d10)

where k denotes the continuum electron, and

Radiative channel	Branching ratio	
$1s^2 2s^2 2p^5 3s^2 3p^6 + \gamma_1$	$\omega(\mathrm{d}\rightarrow\mathrm{d11})=0.115$	(d11)
$1s^2 2s^2 2p^6 3s^2 3p^5 + \gamma_2$	$\omega(\mathrm{d}\rightarrow\mathrm{d12})=0.0092$	(d12)

All the branching ratios given in this example are calculated using Eqs. (1) and (2). States (d1)–(d12) are considered as new parents of the second generation for further decay. The number of intermediate states will rapidly multiply in the second generation, and so forth. Almost all these states have different configurations from each other, and therefore they must be studied individually to get the final-charge-state distribution. The Z and n scaling properties of A_a and A_r are not applicable for most cases because of strong e-e correlations. States (d8), (d9), and (d10) are stable and result in Ar^{2+}, with probability

$$P(\mathrm{Ar}^{2+})=\xi(\mathrm{d}\rightarrow\mathrm{d8})+\xi(\mathrm{d}\rightarrow\mathrm{d9})+\xi(\mathrm{d}\rightarrow\mathrm{d10})$$
$$=0.0007+0.0015+0.0029=0.0051\ .$$

State (d12) gives Ar^{1+}, with probability

$$P(\mathrm{Ar}^{1+})=\omega(\mathrm{d}\rightarrow\mathrm{d12})=0.0092\ ,$$

while states (d1) to (d7) and (d11) are unstable and will decay through Auger emission again. We present in Table I the contribution of each state, from (d1) to (d12), to the final-charge-state distribution, Ar^{1+} to Ar^{6+}.

In order to find the maximum charge state obtainable by cascade decay of a photoexcited atom or ion, the special Auger routes should be found that involve the smallest kinetic energies for the emitted electrons. This allows the most economical way of distributing the original excess energy to the largest number of Auger electrons, taking into account the shell structure of the ions. For $Ar^{+}(\overline{1s})$, we can get Ar^{6+} by the following two routes:

$$(\mathrm{d}\equiv\mathrm{Ar}^{1+})\xrightarrow{A_a}(\mathrm{d1})\xrightarrow{A_a}(\mathrm{x1})\xrightarrow{A_a}(\mathrm{x2})\xrightarrow{A_a}(\mathrm{a,b,c})\xrightarrow{A_a}(\mathrm{f}\equiv\mathrm{Ar}^{6+})$$

and

$$(\mathrm{d}\equiv\mathrm{Ar}^{1+})\xrightarrow{A_a}(\mathrm{d1})\xrightarrow{A_a}(\mathrm{x3})\xrightarrow{A_a}(\mathrm{x4})\xrightarrow{A_a}(\mathrm{a,c})\xrightarrow{A_a}(\mathrm{f}\equiv\mathrm{Ar}^{6+})\ ,$$

where

$$(\mathrm{d})\equiv 1s2s^2 2p^6 3s^2 3p^6,\quad (\mathrm{d1})\equiv 1s^2 2p^6 3s^2 3p^6\ ,$$
$$(\mathrm{x1})\equiv 1s^2 2s 2p^5 3s^2 3p^5,\quad (\mathrm{x2})\equiv 1s^2 2s^2 2p^4 3s^2 3p^4\ ,$$
$$(\mathrm{x3})\equiv 1s^2 2s 2p^5 3s 3p^6,\quad (\mathrm{x4})\equiv 1s^2 2s^2 2p^4 3s 3p^5\ ,$$
$$(\mathrm{a})\equiv 1s^2 2s^2 2p^5 3p^4,\quad (\mathrm{b})\equiv 1s^2 2s^2 2p^5 3s^2 3p^2\ ,$$
$$(\mathrm{c})\equiv 1s^2 2s^2 2p^5 3s 3p^3,\quad (\mathrm{f})\equiv 1s^2 2s^2 2p^6 3p^2\ .$$

The probability of creating Ar^{6+} is then obtained by detailed calculation of all the branching ratios in both these routes; we have

TABLE I. Probabilities P for the charge-state distribution of Ar ions are given for the individual resonance states formed after the first A_a and/or A_r decay. Contributions from all the first-generation resonances are tabulated. The original (d) state $1s2s^2 2p^6 3s^2 3p^6$, was formed by removing the 1s electron to the continuum. Experimental P values from Ref. [3] and also from Ref. [13] are given.

State formed in first generation of decay	Ar^{1+}	Ar^{2+}	Ar^{3+}	Ar^{4+}	Ar^{5+}	Ar^{6+}	Ar^{7+}
(d1)				<0.001	0.020	0.049	
(d2)				0.012	0.189		
(d3)			<0.001	0.013			
(d4)			<0.001	0.017			
(d5)			<0.001	0.482			
(d6)		<0.001	0.018				
(d7)		<0.001	0.072				
(d8) and (d9) (d10)		0.001					
(d11)		0.090	0.024				
(d12)	0.009						
Total	0.009	0.095	0.114	0.524	0.209	0.049	
Expt. (Ref [3])		0.02	0.08	0.41	0.33	0.12	0.04
Expt. (Ref. [13])	0.007	0.10	0.078	0.427	0.25	0.10	0.02

$$P_1(Ar^{6+}) = \xi(d \to d1)\xi(d1 \to x1)\xi(x1 \to x2) \times \xi(x2 \to a,b,c)\xi(a,b,c \to f)$$
$$= (0.0691)(0.637)(0.707)(0.9995)(1)$$
$$= 0.0311$$

and

$$P_2(Ar^{6+}) = \xi(d \to d1)\xi(d1 \to x3)\xi(x3 \to x4) \times \xi(x4 \to a,c)\xi(a,c \to f)$$
$$= (0.0691)(0.273)(0.968)(0.9998)(1)$$
$$= 0.0183$$

and the total probability of Ar^{6+} is the sum of the two probabilities, i.e.,

$$P(Ar^{6+}) = P_1(Ar^{6+}) + P_2(Ar^{6+})$$
$$= 0.0311 + 0.0183$$
$$= 0.0494 .$$

The main computational effort goes into the total widths Γ for the intermediate states, each of which may have more than one decay branch.

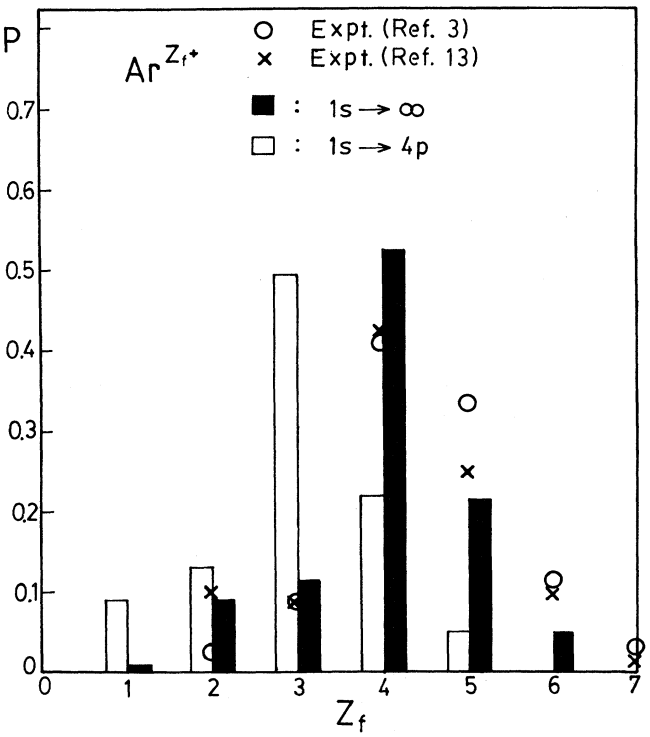

FIG. 1. Probabilities for charge-state distributions are presented, as predicted by the RAC model for Ar ions with the initial $1s \to$ continuum and $1s \to 4p$ excitations. Note the shift in the maximum-charge state, but the overall shape of P is similar in the two cases. Experimental data are from Refs. [3] and [13]. The discrepancy at the high-charge states is presumably due to the neglect of CME processes.

We now compare our results with experiments.[3,13] As summarized in Fig. 1, the agreement is reasonable and the shape of the distribution, which is weighted on the higher-charge side, is reproduced, although theory gives too high a probability for lower-charge states. This is understandable from the approximation we made in the RAC. That is, the configuration averaged A_a tend to ignore some transitions involving small kinetic energies for the continuum electrons. Thus, the Auger channels forbidden in AMA may, in fact, be allowed, and as a result produce higher charge states, such as $1s^2 2s^2 2p^6 3p^6$ and $1s^2 2s^2 2p^6 3s 3p^4$. However, more importantly, sizable contributions from the shake-off, correlated $2e$ transfer, etc. may be present, which have greater effect on the higher charge states, at the level of ± 0.1 in P. Incidentally, we observe that experimental data for Xe show a similar asymmetry in the charge distribution.

IV. OTHER CASES

A. $Ar^{0+}(\overline{1s}, 4p)$

This case is similar to $Ar^{+}(\overline{1s})$, where the initial charge is now shifted down by one, since the $1s$ electron is placed in the $4p$ orbital. We consider here the parent state

$$(d) \equiv 1s 2s^2 2p^6 3s^2 3p^6 4p ,$$

which decays to the following first-generation states:

Auger channel	ξ	
$1s^2 2p^6 3s^2 3p^6 4p$	0.0801	(S1)
$1s^2 2s 2p^5 3s^2 3p^6 4p$	0.196	(S2)
$1s^2 2s 2p^6 3s 3p^6 4p$	0.0157	(S3)
$1s^2 2s 2p^6 3s^2 3p^5 4p$	0.0162	(S4)
$1s^2 2s 2p^6 3s^2 3p^6$	<0.0001	(S5)
$1s^2 2s^2 2p^4 3s^2 3p^6 4p$	0.478	(S6)
$1s^2 2s^2 2p^5 3s 3p^6 4p$	0.0166	(S7)
$1s^2 2s^2 2p^5 3s^2 3p^5 4p$	0.0693	(S8)
$1s^2 2s^2 2p^5 3s^2 3p^6$	<0.0001	(S9)
$1s^2 2s^2 2p^6 3p^6 4p$	0.0007	(S10)
$1s^2 2s^2 2p^6 3s 3p^5 4p$	0.0014	(S11)
$1s^2 2s^2 2p^6 3s 3p^6$	<0.0001	(S12)
$1s^2 2s^2 2p^6 3s^2 3p^4 4p$	0.0029	(S13)
$1s^2 2s^2 2p^6 3s^2 3p^5$	<0.0001	(S14)

Radiative channels	ω	
$1s^2 2s^2 2p^5 3s^2 3p^6 4p$	0.114	(S15)
$1s^2 2s^2 2p^6 3s^2 3p^5 4p$	0.0091	(S16)
$1s^2 2s^2 2p^6 3s^2 3p^6$	<0.0001	(S17)
$1s^2 2s^2 2p^6 3s^2 3p^6 4s$	<0.0001	(S18)
$1s^2 2s^2 2p^6 3s^2 3p^6 3d$	<0.0001	(S19)

The actual calculation is much more involved in this case, as compared to the case discussed in Sec. III, because of the presence of the $4p$ electron which generates additional Auger and radiative channels, as shown above. However, the final-charge-state distribution turned out to be quite similar to that of $Ar^{+}(\overline{1s})$, except for the shift in Z_f by one unit. The reason for this similarity is traced to

TABLE II. Same as Table I, except that the 1s electron is assumed to be removed initially to the 4p orbital.

State formed in first generation of decay	Ar^{0+}	Ar^{1+}	Ar^{2+}	Ar^{3+}	Ar^{4+}	Ar^{5+}
(S1)					0.030	0.050
(S2)			<0.001	0.007	0.189	
(S3)		<0.001	0.016			
(S4)			0.002	0.014		
(S5)			<0.001			
(S6)			<0.001	0.477		
(S7)		<0.001	0.017			
(S8)		<0.001	0.069			
(S9)			<0.0001			
(S10) and (S11)						
(S12) and (S13)		0.005				
(S14)						
(S15)		0.089	0.025			
(S16) and (S17)	0.009					
Total	0.009	0.094	0.129	0.498	0.219	0.050

the fact that there are only a finite number of Auger channels in which the M-shell electrons can be ejected, while more than enough M-shell electrons are available. Any additional electrons in the outer shells do not seriously affect the overall charge-state distribution. We neglect the radiative channels (S18) and (S19) because they are very small. The contribution of each of the first-generation states, (S1) to (S17), to the final-charge-state distribution in this case is shown in Table II. The final result for the charge-state distribution is represented graphically in Fig. 1. The shift down in Z_f by one unit in the charge-state distribution for the case of $Ar(1s,4p)$, from that of $Ar^+(\overline{1s})$, can be easily seen in Fig. 1.

B. $Ar^+(\overline{2s})$

This case is similar to the $Ne(\overline{1s})$ system considered in a previous paper [9], but with the slight additional complication that the $2p \rightarrow 2s$ transition may now be able to eject one of the six electrons in the $3p$ oribtal. We consider for this case the initial parent state

$$(d) \equiv 1s^2 2s 2p^6 3s^2 3p^6$$

and its first generation states created by Auger and radiative decays,

Channel	ξ,ω	
$1s^2 2s^2 2p^5 3s 3p^6$	0.3436	(b1)
$1s^2 2s^2 2p^5 3s^2 3p^5$	0.559	(b2)
$1s^2 2s^2 2p^6 3p^6$	0.0249	(b3)
$1s^2 2s^2 2p^6 3s 3p^5$	0.0691	(b4)
$1s^2 2s^2 2p^6 3s^2 3p^4$	0.0031	(b5)
$1s^2 2s^2 2p^6 3s^2 3p^5$	0.0004	(b6)
$1s^2 2s^2 2p^5 3s^2 3p^6$	<0.0001	(b7)

The radiative channel (b7) has a very small branching ratio and is neglected. States (b3) and (b5) will not decay through Auger emission and give Ar^{2+}, with probability

$$P(Ar^{2+}) = \xi(d \rightarrow b3) + \xi(d \rightarrow b5) = 0.0249 + 0.0031 = 0.028 .$$

States (b1), (b2), and (b4) will decay through Auger emission and the calculation shows that they decay completely to Ar^{3+} with probability

$$P(Ar^{3+}) = [\xi(d \rightarrow b1) + \xi(d \rightarrow b2) + \xi(d \rightarrow b4)] \times \xi(b1, b2, b3 \rightarrow Ar^{3+}) = (0.3436 + 0.5588 + 0.0961)(1) = 0.972 .$$

The final-charge-state distribution of this case is given in Fig. 2(a), and compared with the result of Carlson, Hunt, and Krause [13].

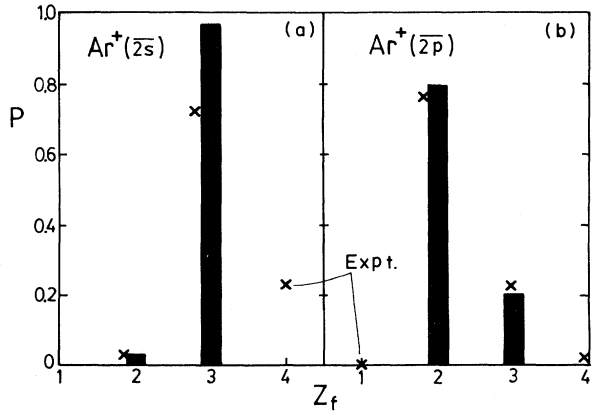

FIG. 2. Same as Fig. 1 but the Ar^+ with a 2s hole (a), and a 2p hole (b). Experimental data of Carlson, Hunt, and Krause (Ref. [13]) are also included.

C. $Ar^+(\overline{2p})$

This case is quite simple, and we have

$$(d)\equiv(1s^2 2s^2)2p^5 3s^2 3p^6 ,$$

which gives the first-generation states

Channel	ξ,ω	
$2p^6 3p^6+e'_1$	$\xi_{11}=0.008$	(d_{11})
$2p^6 3s 3p^5+e'_1$	$\xi_{12}=0.206$	(d_{12})
$2p^6 3s^2 3p^4+e'_1$	$\xi_{12}=0.7854$	(d_{13})
$2p^6 3s 3p^6+\gamma'_1$	$\omega_{14}=0.0002$	(d_{14})

Obviously, (d_{11}) and (d_{13}) result in Ar^{2+} with probability

$$P(Ar^{2+})=\xi(d\rightarrow d_{11})+\xi(d\rightarrow d_{13})=0.008+0.7854$$
$$=0.7934 ,$$

while (d_{13}) decays again and gives Ar^{3+} with probability

$$P(Ar^{3+})=\xi(d\rightarrow d_{12})\xi(d_{12}\rightarrow Ar^{3+})=(0.206)(1)$$
$$=0.206 .$$

The charge-state distribution for $2p$ excitation is shown in Fig. 2(b), where the experimental data of Carlson, Hunt, and Krause [13] are also shown.

V. DISCUSSION AND CONCLUSION

We have applied the simple RAC model to the final-charge-state distribution of Ar. The general feature of the experimental data of Church *et al.* [13] is explained in terms of the initial $1s$ hole configuration. From the result of Sec. IV, where P was calculated for different initial holes, the $2s$ and $2p$ excitations may be responsible for the peak at Ar^{2+}. Improved treatments of some of the transitions involving small transition energies are also desirable.

In previous work [9] on Mg, we noted that the charge-state distributions produced by excitations $1s\rightarrow 3p$ and $1s\rightarrow$continuum are drastically different in their peak values, while no such difference is found between the peak values obtained by the $1s\rightarrow 4p$ and $1s\rightarrow$continuum excitations for Ar. This is attributed to the fact that in Ar more than enough outer-shell electrons are available for Auger emissions. The contribution of the $4p$ channel is small in both radiative and Auger widths, as compared to that of the $2p$ and $3p$ channels. However, in both the Mg and Ar cases the positions of peaks produced by excitation of $1s$ to an upper bound state are shifted down in Z by one unit from that for the $1s$-to-continuum transition.

The RAC model assumes that the shell-structure effect dominates the decay of initial holes, that possible correlated $2e$ processes are small, and that collective multielectron shake-off is not important. For ions with the number of electrons $N\leq 20$, the RAC model seems to be quite effective, but our calculation also shows that the CME effect is not negligible, especially for the higher end of the charge-state distribution (Fig. 1). This is consistent, in both magnitude and shape, with the result found [13] earlier using the simple shake-off model. Much additional work is needed to correctly incorporate the CME effect into the RAC model, and this is under investigation. We note that the CME modes can come in at every stage of the cascade, provided enough energies are available at that stage for multiple electron emission. This fact makes the calculation more difficult.

In addition to the final-charge-state distribution studied here, the Auger and x-ray spectra generated by the cascade decay of hollow ions are also of interest, as they provide further information on the formation of different intermediate states and their decay mechanisms. For example, a recent experimental effort by Levin *et al.* [14] addressed this problem. We are in the process of generating such spectra for the Ar ions [15] using transition probabilities which are already available.

The present work on an 18-electron system, together with our previous work on 10- and 12-electron systems, also shows that the RAC model is probably too cumbersome for systems with $N\geq 20$. A simpler semiquantitative model is under construction to treat more complex systems.

ACKNOWLEDGMENTS

The work reported here was supported in part by the U.S. Department of Energy and by the University of Connecticut. One of us (G.O.) would like to thank the Department of Physics of The University of Connecticut for the hospitality and use of their computer center.

[1] K. W. Jones *et al.*, Comments At. Mol. Phys. **20**, 1 (1987).
[2] F. C. Farnoux, J. Phys. (Paris) Colloq. **49**, C7-3 (1988).
[3] D. A. Church *et al.*, Phys. Rev. A **36**, 2487 (1987); B. M. Johnson *et al.*, Nucl. Instrum. Methods Phys. Res. B **24/25**, 391 (1987).
[4] J. C. Levin, in *Proceedings of the 16th International Conference on the Physics of Electronic and Atomic Collisions, New York, 1989*, edited by A. Dalgarno, R. S. Freund, P. M. Koch, M. S. Lubell, and T. B. Lucatorto (AIP, New York, 1990), p. 176.
[5] P. Zimmermann, Comments At. Mol. Phys. **23**, 45 (1989).
[6] J. P. Briand *et al.*, Phys. Rev. Lett. **65**, 159 (1990).
[7] Y. Hahn, Phys. Lett. **67A**, 345 (1978).
[8] K. J. LaGattuta and Y. Hahn, Phys. Rev. A **25**, 411 (1982).
[9] G. Omar and Y. Hahn, Phys. Rev. A **43**, 4695 (1991).
[10] J. Gau and Y. Hahn, J. Quant. Spectrosc. Radiat. Transfer **23**, 121 (1980).
[11] J. Gau, Y. Hahn, and J. A. Retter, J. Quant. Spectrosc. Radiat. Transfer **23**, 147 (1980).
[12] G. Omar and Y. Hahn, Phys. Rev. A **35**, 918 (1987).
[13] T. A. Carlson, W. E. Hunt, and M. D. Krause, Phys. Rev. **151**, 41 (1966).
[14] J. C. Levin, C. Biedermann, N. Keller, L. Liljeby, C-S. O, R. T. Short, I. A. Sellin, and D. W. Lindle, Phys. Rev. Lett. **65**, 988 (1990).
[15] G. Omar and Y. Hahn (unpublished).